

Lateralized and Region-Specific Thalamic Processing of Lexical Status during Reading Aloud

Dengyu Wang,^{1,2} Witold J. Lipski,¹ Alan Bush,^{3,8} Anna Chrabaszczyk,⁴ Christina A. Dastolfo-Hromack,^{5,6}
 Michael Dickey,⁵ Julie A. Fiez,^{4,7} and R. Mark Richardson^{3,8}

¹Department of Neurological Surgery, University of Pittsburgh School of Medicine, Pittsburgh, Pennsylvania 15213, ²School of Medicine, Tsinghua University, Beijing 100084, China, ³Brain Modulation Lab, Massachusetts General Hospital, Boston, Massachusetts 02114, ⁴Department of Psychology, University of Pittsburgh, Pittsburgh, Pennsylvania 15213, ⁵Department of Communication Science and Disorders, University of Pittsburgh, Pittsburgh, Pennsylvania 15213, ⁶Department of Communication Science and Disorders, West Virginia University, Morgantown, West Virginia 26506, ⁷Brain Institute, University of Pittsburgh, Pittsburgh, Pennsylvania 15213, and ⁸Harvard Medical School, Harvard University, Boston, Massachusetts 02115

To explore whether the thalamus participates in lexical status (word vs nonword) processing during spoken word production, we recorded local field potentials from the ventral lateral thalamus in 11 essential tremor patients (three females) undergoing thalamic deep-brain stimulation lead implantation during a visually cued word and nonword reading-aloud task. We observed task-related beta (12–30 Hz) activity decreases that were preferentially time locked to stimulus presentation, and broadband gamma (70–150 Hz) activity increases, which are thought to index increased multiunit spiking activity, occurring shortly before and predominantly time locked to speech onset. We further found that thalamic beta activity decreases bilaterally were greater when nonwords were read, demonstrating bilateral sensitivity to lexical status that likely reflects the tracking of task effort; in contrast, greater nonword-related increases in broadband gamma activity were observed only on the left, demonstrating lateralization of thalamic broadband gamma selectivity for lexical status. In addition, this lateralized lexicality effect on broadband gamma activity was strongest in more anterior thalamic locations, regions which are more likely to receive basal ganglia than cerebellar afferents and have extensive connections with prefrontal cortex including Brodmann's areas 44 and 45, regions consistently associated with grapheme-to-phoneme conversions. These results demonstrate active thalamic participation in reading aloud and provide direct evidence from intracranial thalamic recordings for the lateralization and topography of subcortical lexical status processing.

Key words: deep brain stimulation; language; lexicality effect; local field potential; reading aloud; thalamus

Significance Statement

Despite the corticocentric focus of most experimental work and accompanying models, there is increasing recognition of the role of subcortical structures in speech and language. Using local field potential recordings in neurosurgical patients, we demonstrated that the thalamus participates in lexical status (word vs nonword) processing during spoken word production, in a lateralized and region-specific manner. These results provide direct evidence from intracranial thalamic recordings for the lateralization and topography of subcortical lexical status processing.

Received June 25, 2021; revised Jan. 14, 2022; accepted Jan. 14, 2022.

Author contributions: D.W., W.J.L., and R.M.R. designed research; D.W., W.J.L., and R.M.R. performed research; A.B., M.D., and J.A.F. contributed unpublished reagents/analytic tools; D.W., W.J.L., A.B., A.C., C.A.D.-H., and J.A.F. analyzed data; D.W. and R.M.R. wrote the paper.

This work was supported by National Institutes of Health Grant U01NS098969 (R.M.R.), the Hamot Health Foundation (R.M.R.), a University of Pittsburgh Brain Institute NeuroDiscovery Pilot Research Award (R.M.R.), and the University of Pittsburgh-Tsinghua University Scholars Program (D.W.).

The authors declare no competing financial interests.

Correspondence should be addressed to Witold J. Lipski atlipskiw@upmc.edu or R. Mark Richardson at mark.richardson@mgh.harvard.edu.

<https://doi.org/10.1523/JNEUROSCI.1332-21.2022>

Copyright © 2022 the authors

Introduction

Reading words aloud depends on our ability to transform information about letter combinations into plans for producing speech sounds. Although word reading can be supported by processes that permit mapping entire word forms to lexical representations, nonword reading depends on sublexical processes that map spelling and sound (Coltheart et al., 2001). Functional neuroimaging has allowed for an increasingly detailed study of the cortical regions that participate in these phonological processes, for instance, demonstrating that a region of the inferior frontal gyrus (IFG, Brodmann's areas 44 and 45) is significantly more active for nonword reading than for word reading

(Herbster et al., 1997; Fiez et al., 1999; Hagoort et al., 1999; Heim et al., 2005). Subcortical involvement in speech and language, however, is not well understood. Although thalamic activation during word reading tasks has been reported (Bookheimer et al., 1995; Cohen et al., 2002; Fiebach et al., 2002; Seghier and Price, 2010), the relatively low spatial resolution and indirect nature of imaging techniques for assessing subcortical neural activation represent fundamental limitations (Llano, 2013). Resolving this knowledge gap is important, given that cortical activity is modulated by thalamic outflow through basal ganglia-thalamo-cortical and cerebello-thalamo-cortical circuits (Behrens et al., 2003; Zhang et al., 2010; Bosch-Bouju et al., 2013; Hwang et al., 2017).

Neurosurgical procedures involving invasive recording and stimulation in epilepsy patients undergoing electrode implantation for seizure mapping traditionally have provided the only direct means to test hypotheses related to cortical function during reading. Epilepsy surgery, however, rarely provides access to subcortical structures. Movement disorders surgery, on the other hand, routinely provides direct access to subcortical structures, including the thalamus. Although the ventral lateral posterior nucleus of the thalamus (VLP) mainly relays information between the cerebellum and the primary motor cortex, the ventral lateral anterior nucleus (VLa) and ventral anterior nucleus (VA) primarily receive inputs from the internal globus pallidus and substantia nigra pars reticulata, and have extensive connections with prefrontal cortex, including Broca's area (Alexander et al., 1986; Behrens et al., 2003; Zhang et al., 2010; Bosch-Bouju et al., 2013; Hwang et al., 2017; Hintzen et al., 2018); both regions are encountered during implantation of deep brain stimulation (DBS) leads into the ventral intermediate nucleus of the thalamus (Vim), which corresponds to the ventral portion of the VLP (Macchi and Jones, 1997). Regionalization of language function within the left ventral lateral thalamus was established in surgery for movement disorders in the 1970s in seminal studies by Johnson and Ojemann (2000), which used electrical stimulation principles borrowed from traditional cortical language mapping protocols. However, intracranial thalamic electrophysiology collected during spoken word production is still rare, which limits further understanding of a thalamic role in language processing.

We recently developed a protocol to study subcortical activity during single-syllable word/nonword reading in patients undergoing DBS lead implantation in the subthalamic nucleus to treat symptoms of Parkinson's disease (Lipski et al., 2018; Chrabaszcz et al., 2019). We expanded this paradigm to investigate thalamic involvement in speech production and language processing by recording local field potentials (LFP) in patients undergoing Vim DBS lead implantation for essential tremor. Subjects performed a reading-aloud task where they were asked to read aloud single-syllable words or nonwords that appeared on a computer screen. We focused our analysis on beta (12–30 Hz) and broadband gamma (70–150 Hz) LFPs; beta oscillations have been proposed to signal maintenance of current sensorimotor or cognitive states (Engel and Fries, 2010), and broadband gamma activity correlates well with multiunit neuronal spiking (Ray et al., 2008; Ray and Maunsell, 2011). We expected to observe thalamic beta activity decreases and broadband gamma activity increases during the task, in line with the existing data on neural power modulations during voluntary movements (Crone et al., 1998a,b). We further explored lexicality effect and its lateralization within the ventral lateral thalamus by comparing thalamic LFPs when participants spoke words versus nonwords.

Materials and Methods

Subjects. Participants included 11 human subjects (three females, 53–84 years old with a median age of 68) with essential tremor undergoing awake DBS implantation surgery targeting the Vim nucleus of the thalamus. All participants were right-handed native English speakers. None had significant cognitive impairment based on a detailed neuropsychological evaluation performed during clinical evaluation for DBS surgery. All but one underwent bilateral (left side first) DBS lead implantation (One subject had one lead implanted in the left hemisphere previously and underwent right-side lead implantation in the current study.). A full demographic description of subjects is provided in Table 1. All protocols were approved by the Institutional Review Board of the University of Pittsburgh (Protocol No. PRO13110420), and all participants gave written informed consent.

Stimuli and experimental paradigm. Subjects performed a reading-aloud task either during the subcortical mapping portion of the surgery (4/11 subjects with mapping electrode recordings) or after the placement of DBS lead in each side (7/11 subjects with lead electrode recordings). For the four subjects with mapping electrode recordings, each subject performed up to four task sessions, and the seven subjects with lead electrode recordings each performed two task sessions (The first session occurred after left lead was implanted, and the second session took place after bilateral implantation was completed.). Each session included 120 trials. The stimuli were consonant-vowel-consonant (CVC) words and nonwords that were presented on a computer screen. Four lists of 120 stimuli were constructed based on a previous work (Moore et al., 2017). The first 60 stimuli of each list alternated between unique words and nonwords, and those words and nonwords were balanced along a number of psycholinguistic features, including phoneme probability, phonological neighborhood density, bigram frequency, and biphone probability. The nonwords were duplicated twice to construct the last 60 stimuli of each list. One of the four stimulus lists was presented to the subjects during each task session. For lexicality (word vs nonword) related analyses, only the first 60 trials of each session were used.

The experimental paradigm was programmed using MATLAB (MathWorks) and Psychophysics Toolbox extensions (Brainard, 1997). A schematic of the experiment is shown in Figure 1. Before each trial, a white fixation cross was presented on the screen. Each trial was initiated manually by the experimenter, with the appearance of a green fixation cross on the screen. The green fixation cross lasted 250 ms and was followed by a variable time delay (500–1000 ms), during which the screen remained black. Then the CVC syllable stimulus was presented in white on the screen, and subjects were instructed to read it aloud. The text remained on the screen until the subjects finished speaking. A white fixation cross was presented on the screen during the intertrial interval (618 ± 302 ms).

Electrophysiological recordings. For the 4/11 subjects where physiological subcortical mapping was administered, LFP recordings were performed using the Neuro Omega recording system (Alpha Omega) and mapping electrodes that have a stainless steel macroelectrode ring (0.55 mm in diameter, 1.4 mm in length) 3 mm above the tip, whereas in the other 7/11 subjects, LFP signal was recorded from Medtronic Model 3387 DBS leads (model 3387) with four platinum-iridium electrodes (1.27 mm in diameter, 1.5 mm in length), spaced 1.5 mm apart, using Grapevine Neural Interface Processor (Ripple). The mapping electrodes and the DBS leads targeted the Vim. For subjects with mapping electrode recordings, three mapping electrodes were placed in three trajectories (anterior, central, and posterior trajectories, or central, posterior, and medial trajectories) of a standard cross-shaped Ben-Gun array with a 2 mm center-to-center spacing, and made simultaneous recordings starting at 15 mm above the surgical target with manual advance in 0.1 mm steps. The reading-aloud task was conducted in pauses during subcortical mapping procedure and subjects performed in up to four recording sessions, with each session corresponding to a different recording depth. Mapping electrode recordings were performed only during the left-side implantation except for one subject who underwent unilateral implantation in the right side, and thus got mapping electrode recordings only in the right side. For subjects with DBS lead electrode

Table 1. Subject characteristics

Subject	Age	Gender	MMSE	LFP recording side	LFP recording type	Number of sessions	Number of recordings	Mean number of trials per session	Trials rejected (%)
1	61	Male	NR	Left	Mapping electrodes	4	12	111	7
2	70	Female	30/30	Right	Mapping electrodes	2	6	107	11
3	66	Male	NR	Left	Mapping electrodes	2	6	116	3
4	75	Male	26/30	Left	Mapping electrodes	3	9	112	5
5	64	Male	30/30	Both	DBS leads	2	12	104	13
6	53	Male	NR	Both	DBS leads	2	12	113	5
7	67	Male	26/30	Both	DBS leads	2	12	111	7
8	71	Male	26/30	Both	DBS leads	2	12	108	9
9	84	Female	30/30	Both	DBS leads	2	12	118	2
10	73	Female	30/30	Both	DBS leads	2	12	109	9
11	68	Male	28/30	Both	DBS leads	2	12	114	5

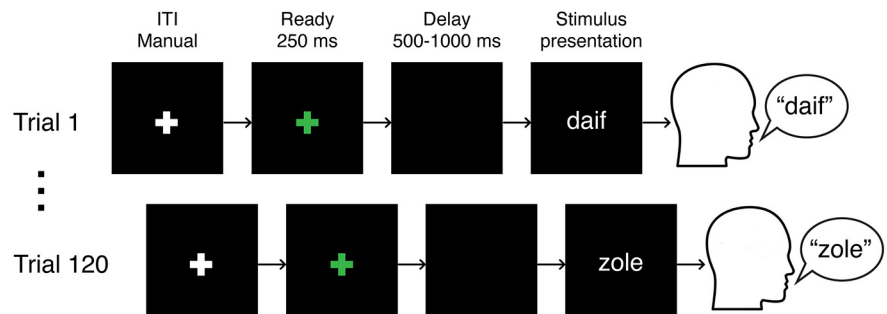
MMSE, Mini Mental State Examination; NR, not recorded.

recordings, the task was administered in two recording sessions, one after the implantation of the DBS lead in the left side, receiving recordings from only the left DBS lead electrodes, and the other after bilateral DBS lead implantation was completed, receiving simultaneous recordings from bilateral lead electrodes. The LFP signal recorded from mapping electrodes was sampled at 44 kHz and bandpass filtered from 0.075 Hz to 10 kHz, and data recorded from DBS lead electrodes were collected at 30 kHz. Signal collected in one recording site in one session counted as one recording. Subject recording characteristics are summarized in Table 1.

Audio recordings. Subjects' speech signal was recorded using an omnidirectional microphone (model ATR3350iS, frequency response 50–18,000 Hz, Audio-Technica) for six subjects, and a Precision Flat Frequency PRM1 microphone (frequency response 20–20,000 Hz for five subjects, PreSonus) placed ~8 cm away from the subject's mouth and oriented at an angle of ~45°. The audio signal was collected by Grapevine Neural Interface Processor at a sampling frequency of 30 kHz. For subjects with mapping electrode recordings, the audio signal was then synchronized with neural signal recorded by the Neuro Omega system using digital pulses delivered to both recording systems via a USB data acquisition unit (catalog #USB-1208FS, Measurement Computing).

Electrode localization. DBS lead electrodes and mapping electrodes were localized using LEAD-DBS toolbox (Horn and Kühn, 2015; Horn et al., 2019). Postoperative brain scans were coregistered to preoperative brain scans using open-source Advanced Normalization Tools. Preoperative and postoperative acquisitions were then normalized into Montreal Neurologic Institute (MNI) ICBM152 NLIN 2009b stereotactic space (Fonov et al., 2011). Both coregistration and normalization results underwent a manual quality check. Semiautomatic reconstruction of electrodes in MNI space was performed in LEAD-DBS, and MNI-defined coordinates were determined for all the electrode contacts (Fig. 2). A digitized and normalized to MNI space version of the Ewert atlas (Ewert et al., 2018) was used to categorize the electrode contacts. A contact was assigned to a nucleus if it was within or in the vicinity of the nucleus (1 mm cutoff) based on the minimum Euclidean distance between the contact and the voxels of the nucleus.

Data preprocessing. The audio signal was segmented into trials, and the speech sound was coded by a speech-language pathologist in a custom-designed graphical user interface implemented in MATLAB. Coding was based on acoustic evidence of speech features and articulator movements for the phonemes produced, which were visualized with broadband spectrograms. For example, plosive onset was marked at the rapid increase of high-frequency energy associated with the burst release. For each trial, (1) the onset of speech, (2) the offset of speech, and (3) the speech content were identified. Trials were considered correct and included in further analyses if they met all the following criteria: (1) the subject's speech response could be clearly identified by the coder, (2) the

**Figure 1.** Schematic of experiment.

subject's response was the targeted CVC syllable without prereponse and postresponse vocalizations, and (3) the response did not make a nonword into a word or make a word into a nonword.

Electrophysiological data were preprocessed using custom code based on the FieldTrip toolbox (Oostenveld et al., 2011) in MATLAB. The data were resampled at 1 kHz and bandpass filtered from 2 to 400 Hz. The data were also notch filtered at 60 Hz and its harmonics to remove line noise. Time series data from all recording sites were visually and quantitatively inspected for quality control. The data were then segmented into trials, each spanning 2 s before stimulus presentation to 2 s after the end of speech. Trials with artifacts or excessive noise were identified both manually and quantitatively and were excluded for subsequent analyses. Combined with trials that did not meet the criteria for correct speech responses (see above), an average $6.9 \pm 3.4\%$ of trials per subject were rejected (Table 1). The remaining data were common-average referenced to minimize noise. For spectral-temporal analysis, the data were decomposed using Morlet wavelet transformation (width = 7) over frequencies of 2–200 Hz in increment steps of 2 Hz. For band activity analyses, instantaneous analytic amplitudes of beta and broadband gamma frequency bands were extracted from respective bandpass filters using Hilbert transform. The resulting signal of each trial was z-scored relative to the baseline (a period of 1000 ms preceding stimulus presentation).

Task-related responses. Time-frequency data were averaged across all trials centering on speech onset (from 2 s before speech onset to 2 s after speech onset), z-scored to baseline, and then averaged across all recordings. A nonparametric two-tailed Wilcoxon signed-rank test was performed to determine time windows of significant time-frequency modulations compared with baseline. Significant time windows for beta and broadband gamma were then used to calculate a mean beta response strength and mean broadband gamma response strength for each trial in each recording, respectively. Then a one-tailed one-sample *t* test was performed on each recording to determine recordings that had significant beta activity decreases and recordings that had significant broadband gamma activity increases, respectively.

Locking analysis. In an effort to characterize the timing properties of beta decrease response and broadband gamma increase response for

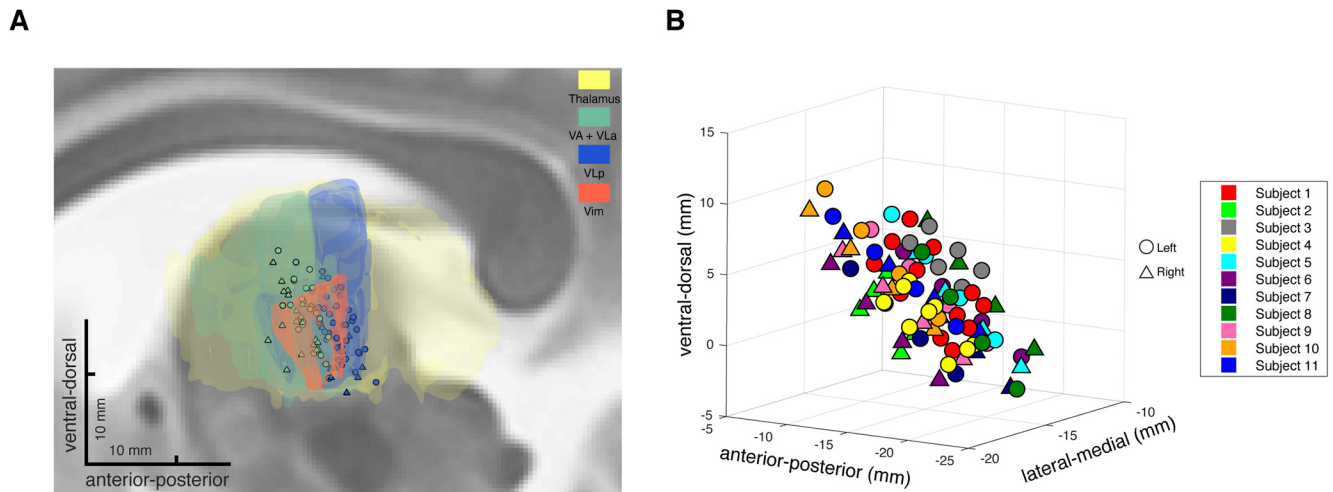


Figure 2. Localization and MNI transformation of recording sites. **A**, Sagittal view of the recording locations of all the subjects relative to the thalamus (yellow), VA, and VL (green), VLp (blue), and Vim (orange), superimposed on a T2-weighted image. Recording locations are color coded based on the nuclei they were assigned to. **B**, A plot of all the recording sites in MNI space with their MNI-defined coordinates. Recording contacts of different subjects are color coded. In both **A** and **B**, right hemisphere recording locations are flipped to the left hemisphere; left side contacts are marked with circles, and right side contacts are marked with triangles.

recordings with significant task-related changes in either band activity, we examined the trial-to-trial relationships of significant band response onsets to stimulus presentation versus speech onset in these recordings. First, beta or broadband gamma time series data of each trial were smoothed using a moving average kernel of 200 ms and z -scored to baseline to minimize single-trial noise. For recordings with significant beta decrease responses, a thresholding method with a critical value of $z = -1.645$ was applied to determine the onset of beta response for each trial. Specifically, for each trial, the period with band response power below the threshold that gave minimum summed activity was considered as activation period, and the beginning of the period was determined as onset of beta response. For recordings with significant broadband gamma increase responses, the onset of broadband gamma increase was determined in a similar way, except that a critical value of $z = 1.645$ was used, and period of maximum summed activity above the threshold was considered as activation period. For each band, a trial of one recording was discarded for locking analysis if no beyond-threshold period was present throughout the trial. The following intervals were calculated for each trial: (1) the interval between stimulus presentation and the onset of significant band response (band response latency) and (2) the interval between the onset of significant band response and the onset of speech (band response onset to speech onset interval). Then the two intervals were correlated (Pearson's correlation) with speech production latency (interval between stimulus presentation and onset of speech) across trials for each recording, respectively. The band response of a recording was considered to be more time locked to stimulus presentation if (1) band response onset to speech onset interval was significantly correlated with speech production latency, and (2) the correlation coefficient (Pearson's r) between band response onset to speech onset interval and speech production latency was greater than the correlation coefficient between band response latency and speech production latency. On the contrary, the band response was considered to be more time locked to speech onset if (1) band response latency was significantly correlated with speech production latency, and (2) the correlation coefficient between band response latency and speech production latency was greater than the correlation coefficient between band response onset to speech onset interval and speech production latency. If a band response did not meet either of the two criteria, it was considered not locked to either stimulus presentation or speech onset. A schematic illustrating stimulus-locked and speech-locked neural response types is provided in Figure 3.

Lexical status selectivity analysis. We used the first 60 trials of recordings that were from the seven subjects with bilateral data and that showed significant task-related modulations in beta or broadband gamma activity to make comparisons between the left and right

thalamus in terms of lexical status (word vs nonword) selectivity of band activity. To depict time-resolved band responses during word versus nonword trials, a mean z -scored band response curve averaged across trials and across recordings was obtained for each frequency band, each trial type (word/nonword), in each side. Response curves were aligned to stimulus presentation for beta and aligned to speech onset for broadband gamma, based on their respective locking properties. Periods of significant differences between word-related responses and nonword-related responses were determined with a two-tailed paired t test using a sliding window of 100 ms.

To quantify the extent of band response difference between word and nonword trials at single recording level, beta lexical status selectivity indexes and broadband gamma lexical status selectivity indexes were calculated for respective recordings. For each recording, the mean response power values of a particular frequency band over the corresponding significant time window determined before (see above, Task-related responses; see Fig. 5) were calculated for word trials and nonword trials. A two-sample t test was then performed between nonword-related power values and word-related power values, and the resulting t statistic was the lexical status selectivity index of that frequency band for that recording. For beta, a lexical status selectivity index smaller than zero meant that the recording showed stronger beta activity decrease (thus having more negative z -scored power) during nonword trials than during word trials and vice versa. For broadband gamma, a lexical status selectivity index greater than zero indicated that the recording showed stronger broadband gamma activity increase during nonword reading aloud than during word reading aloud and vice versa. A recording location was considered significantly nonword-selective if lexical status selectivity index was smaller than -1.645 for beta activity or >1.645 for broadband gamma activity (normal approximation of t distribution).

Statistical analysis. All statistical analyses were performed in MATLAB R2017b. Comparisons between sample mean and zero were made using one-tailed or two-tailed one-sample t tests, as appropriate. Between-group comparisons were made using two-tailed paired or unpaired t tests. Association between two categorical variables was examined with a χ^2 test. The relationship between two continuous variables was measured using a Pearson's correlation test. Stepwise linear regression models were used to test out possible variable interactions and minimize multicollinearity. Linear mixed-effects models were applied to control for confounding factors (MATLAB function fitglme with the following formula: response variable \sim independent variable + (1 | confounding factor A) + (1 | confounding factor B) + ...). Statistical methods that are associated with specific analyses are stated in previous sections. Continuous data were presented as mean \pm SD unless

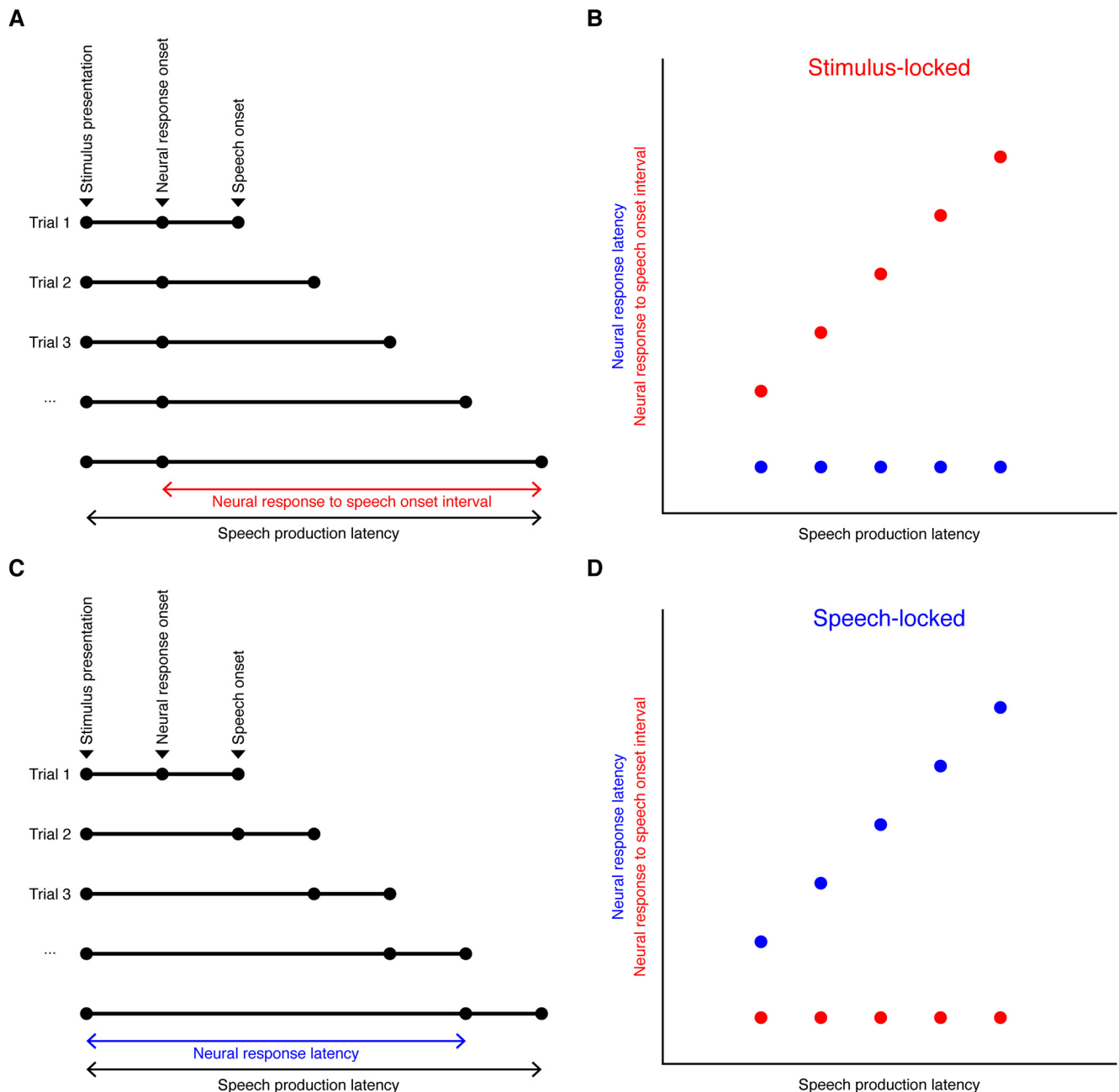


Figure 3. Schematic illustrating stimulus-locked and speech-locked neural response types. **A, B**, An example of neural responses that are perfectly time locked to stimulus presentation, with constant neural response latency despite varying speech production latency. **C, D**, An example of neural responses that are perfectly time locked to speech onset, with constant neural response onset to speech onset interval despite varying speech production latency.

otherwise stated. Statistical significance was defined as $p < 0.05$. Bonferroni's correction was applied for multiple comparisons. No explicit power analysis was performed as no effect size of thalamic neural modulations during spoken word production has been previously reported. Our results are based on 117 LFP recordings collected from 11 subjects, a sample size that is in accordance with previous subcortical recording studies (Brücke et al., 2013; Lipski et al., 2018; Chrabaszcz et al., 2019).

Data availability. Data and code reproducing the results are available at <https://github.com/Brain-Modulation-Lab/VimLexicality>.

Results

A total of 117 recordings from 89 recording sites pooled across subjects were collected (Table 1). Recording locations were determined

to be within or bordering (within 1 mm) the VA and VLa (38/89) or the VLp (51/89; Fig. 2). Across all subjects, the mean speech production latency (interval between stimulus presentation and onset of speech) was 1.02 ± 0.55 s, and the mean duration of speech (interval between speech onset and speech offset) was 0.69 ± 0.21 s. Nonword production latency was significantly longer than word production latency (1.16 ± 0.73 s vs 0.93 ± 0.43 s; linear mixed effects model with subject and session as random effects, estimated coefficient = 0.23, SE = 0.027, $p < 10^{-5}$), and nonword production duration was slightly but significantly longer than word production duration (0.71 ± 0.23 s vs 0.67 ± 0.19 s; linear mixed-effects model with subject and session as random effects, estimated coefficient = 0.041, SE = 0.010, $p = 4.8 \times 10^{-5}$). Distributions of speech production latency and speech duration are shown in Figure 4.

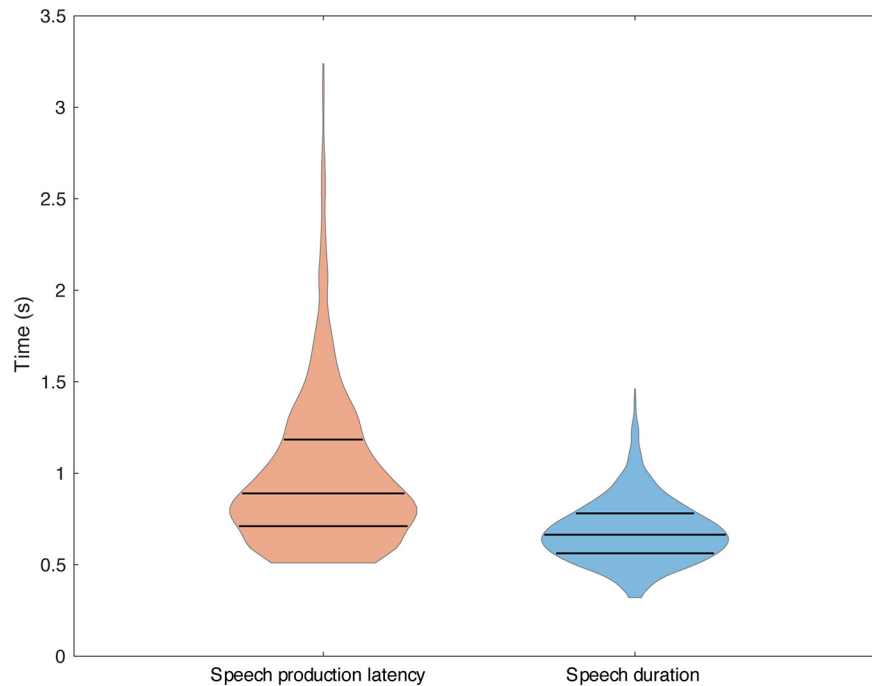


Figure 4. Distributions of behavioral outcomes. Violin plots showing the distributions of speech production latency and speech duration, respectively. The lower quartile, the median, and the upper quartile are marked with horizontal lines.

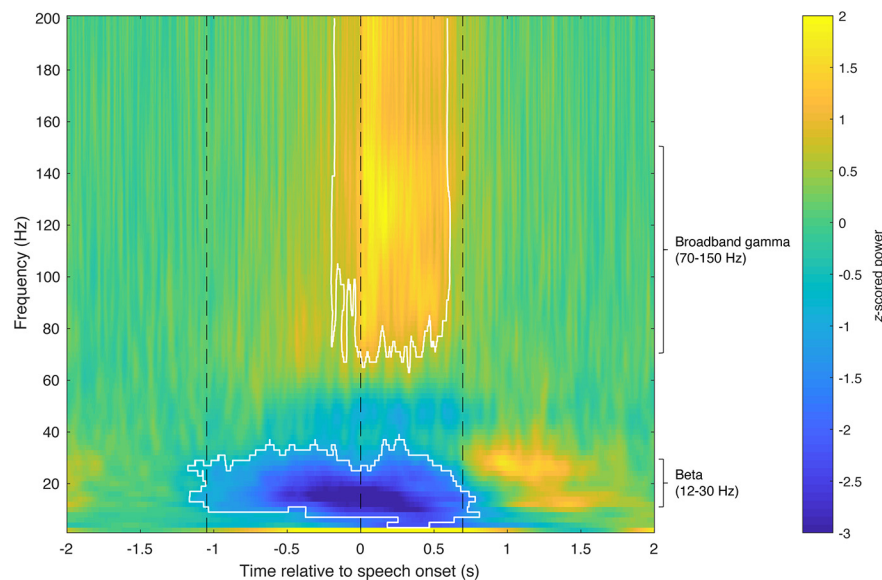


Figure 5. Thalamic neural activity shows task-related modulations. A spectrogram of thalamic neural activity during the reading-aloud task, averaged across all trials and all recordings. Trials are aligned to speech onset. Significant changes compared with baseline are marked in white contours (-1.08 – 0.62 s for beta activity, and -0.15 – 0.59 s for broadband gamma activity; Wilcoxon signed-rank test, $n = 117$, $p < 0.05$, Bonferroni corrected for multiple comparisons across frequency bins and time points). Average time points of stimulus presentation and speech onset and offset are marked with black dashed lines.

Thalamic neural activity is modulated during reading aloud

Thalamic LFP activity exhibited significant time-frequency modulation during the reading-aloud task (Fig. 5). Compared with baseline, there was a significant decrease in spectral power in the beta frequency band that occurred at stimulus presentation and lasted until the end of speech (-1.08 – 0.62 s relative to speech onset; two-tailed Wilcoxon signed-rank test, $n = 117$, $p < 0.05$, Bonferroni corrected for multiple comparisons across frequency bins and time points). A beta power rebound was observed following the offset of speech. In contrast, a significant increase in

broadband gamma activity occurred shortly before the onset of speech and persisted throughout the utterance (-0.15 – 0.59 s relative to speech onset; two-tailed Wilcoxon signed-rank test, $n = 117$, $p < 0.05$, Bonferroni corrected for multiple comparisons across frequency bins and time points). Increased oscillatory activity in the delta frequency range (1–4 Hz) was also observed during the task. Average z-scored task-related beta and broadband gamma response amplitudes of each trial were then calculated over the respective significant time windows for all the recordings. As a result, 66/117 (56%) of the recordings showed

significant beta activity decreases during the task compared with baseline (one-tailed one-sample t test, $p < 0.05$, Bonferroni corrected for multiple comparisons across the recordings), and significant task-related broadband gamma activity increases were observed in 91/117 (78%) of the recordings (one-tailed one-sample t test, $p < 0.05$, Bonferroni corrected for multiple comparisons across the recordings).

Beta and broadband gamma responses differ in timing properties

The average interval between stimulus presentation and onset of a significant change from baseline in the spectral power of a particular frequency band, that is, the mean band response latency, was shorter for significant beta decrease responses than for significant broadband gamma increase responses (0.79 ± 0.18 s vs 0.99 ± 0.18 s; two-tailed two-sample t test, $t_{(155)} = -6.97$, Cohen's $d = -1.12$, $p < 10^{-5}$). The mean band response onset to speech onset interval was also greater for significant beta decrease responses than for significant broadband gamma increase responses (0.31 ± 0.15 s vs 0.13 ± 0.14 s; two-tailed two-sample t test, $t_{(155)} = 7.67$, Cohen's $d = 1.23$, $p < 10^{-5}$). To characterize the temporal properties of these responses, we examined their trial-to-trial relationships to stimulus presentation versus speech onset (Fig. 6A–D). Of the 66 recordings that showed significant task-related beta power decreases, 43 (65.2%) had beta responses time locked to stimulus presentation, whereas only 19 (28.8%) had beta responses time locked to speech onset (Fig. 6E). In contrast, the majority (70/91, 77.0%) of significant broadband gamma power increases were time locked to speech onset, with a minority (19/91, 21.0%) time locked to stimulus presentation (Fig. 6F). These relationships were dissociated, with beta decreases more likely to be stimulus locked (χ^2 test, $\chi^2(1) = 31.4$, Cohen's $\omega = 0.45$, $p < 10^{-5}$) and broadband gamma increases more likely to be speech onset locked (χ^2 test, $\chi^2(1) = 36.1$, Cohen's $\omega = 0.48$, $p < 10^{-5}$). These temporal correlations did not differ between recording sides (χ^2 test, beta decrease response: $\chi^2(2) = 1.50$, Cohen's $\omega = 0.15$, $p = 0.47$; broadband gamma increase response: $\chi^2(2) = 2.49$, Cohen's $\omega = 0.17$, $p = 0.29$).

Thalamic beta activity is modulated by lexicality bilaterally

To investigate the involvement and lateralization of the thalamus in lexical status (word vs nonword) processing, only recordings that were from subjects with bilateral lead recordings ($n = 7$) and that showed significant task-related modulations in beta or broadband gamma activity were included for lexicality-related analyses. As a result, 55 recordings [21 unilateral session left-side recordings, 34 from bilateral session left-side (20) or right-side (14) recordings] were included for beta lexical status selectivity analysis. Nonword reading was associated with a greater suppression of beta power compared with word reading. These differential beta responses were observed in both hemispheres (Fig. 7A,C). In the left thalamus, significant word versus nonword beta amplitude differences occurred between 0.8 and 1.8 s after stimulus presentation (two-tailed paired t test, $n = 41$, $p < 0.05$, Bonferroni corrected for multiple comparisons across time bins). Similarly, significant beta amplitude differences occurred in the right thalamus at 0.2–1.7 s relative to stimulus presentation (two-tailed paired t test, $n = 14$, $p < 0.05$, Bonferroni corrected for multiple comparisons across time bins).

The mean beta lexical status selectivity indexes for unilateral session left-side recordings (-0.49 ± 0.76) and bilateral session left-side (-0.52 ± 0.82) and right-side (-0.82 ± 0.89)

recordings were all significantly less than zero (two-tailed one-sample t test, $t_{(20)} = -2.97$, Cohen's $d = -0.65$, $p = 0.0075$; $t_{(19)} = -2.83$, Cohen's $d = -0.63$, $p = 0.011$; $t_{(13)} = -3.48$, Cohen's $d = -0.93$, $p = 0.0041$; Fig. 7E), suggesting that the magnitude of the beta decrease was significantly nonword selective in each case. There were no significant differences in beta lexical status selectivity between recordings in the left and right thalamus or between recordings from the unilateral and bilateral sessions on the left side (two-tailed two-sample t test, unilateral session left-side recordings vs bilateral session right-side recordings: $t_{(33)} = 1.18$, Cohen's $d = 0.41$, $p = 0.25$; bilateral session left-side recordings vs bilateral session right-side recordings: $t_{(32)} = 1.05$, Cohen's $d = 0.37$, $p = 0.30$; unilateral session left-side recordings vs bilateral session left-side recordings: $t_{(39)} = 0.093$, Cohen's $d = 0.03$, $p = 0.93$).

Thalamic broadband gamma activity is modulated by lexicality in the left hemisphere

Seventy-four recordings (26 unilateral session left-side recordings, 22 bilateral session left-side recordings, and 26 bilateral session right-side recordings) were included for broadband gamma lexical status selectivity analysis. Significantly greater broadband gamma activity increases during nonword production were observed in the left thalamus, starting 0.1 s after speech onset and persisting throughout the following 0.4 s (two-tailed paired t test, $n = 48$, $p < 0.05$, Bonferroni corrected for multiple comparisons across time bins; Fig. 7B). In the right thalamus, however, the broadband gamma response curves observed during nonword and word reading were similar, without a significant difference in response amplitudes (two-tailed paired t test, $n = 26$, Bonferroni corrected for multiple comparisons across time bins; Fig. 7D).

The mean broadband gamma lexical status selectivity indexes of both unilateral session left-side recordings (0.53 ± 0.96) and bilateral session left-side recordings (0.46 ± 1.00) were significantly greater than zero (two-tailed one-sample t test, $t_{(25)} = 2.80$, Cohen's $d = 0.55$, $p = 0.0097$; $t_{(21)} = 2.14$, Cohen's $d = 0.46$, $p = 0.044$), indicating significant association between nonword reading and stronger broadband gamma activation (Fig. 7F). In contrast, broadband gamma responses in right side recordings did not show significant lexical status selectivity (-0.22 ± 0.68 ; two-tailed one-sample t test, $t_{(25)} = -1.67$, Cohen's $d = -0.33$, $p = 0.11$). The differences in broadband gamma lexical status selectivity between the left and right thalamus were demonstrated with two-tailed two-sample t test (unilateral session left-side recordings vs bilateral session right-side recordings: $t_{(50)} = 3.25$, Cohen's $d = 0.92$, $p = 0.0021$; bilateral session left-side recordings vs bilateral session right-side recordings: $t_{(46)} = 2.79$, Cohen's $d = 0.82$, $p = 0.0077$), further suggesting that selectivity of thalamic broadband gamma activity to lexical status is lateralized to the left. Recordings in the unilateral and bilateral sessions on the left side did not differ in broadband gamma lexical status selectivity (two-tailed two-sample t test, $t_{(46)} = 0.25$, Cohen's $d = 0.074$, $p = 0.80$), indicating the consistency of broadband gamma lexical status selectivity between task sessions.

Left-side broadband gamma lexical status selectivity is topographically organized

We observed that the recording sites in the left thalamus that were significantly nonword selective in terms of broadband gamma response activity (broadband gamma lexical status selectivity index greater than 1.645 based on normal approximation of t distribution) appeared to have more anterior locations in MNI

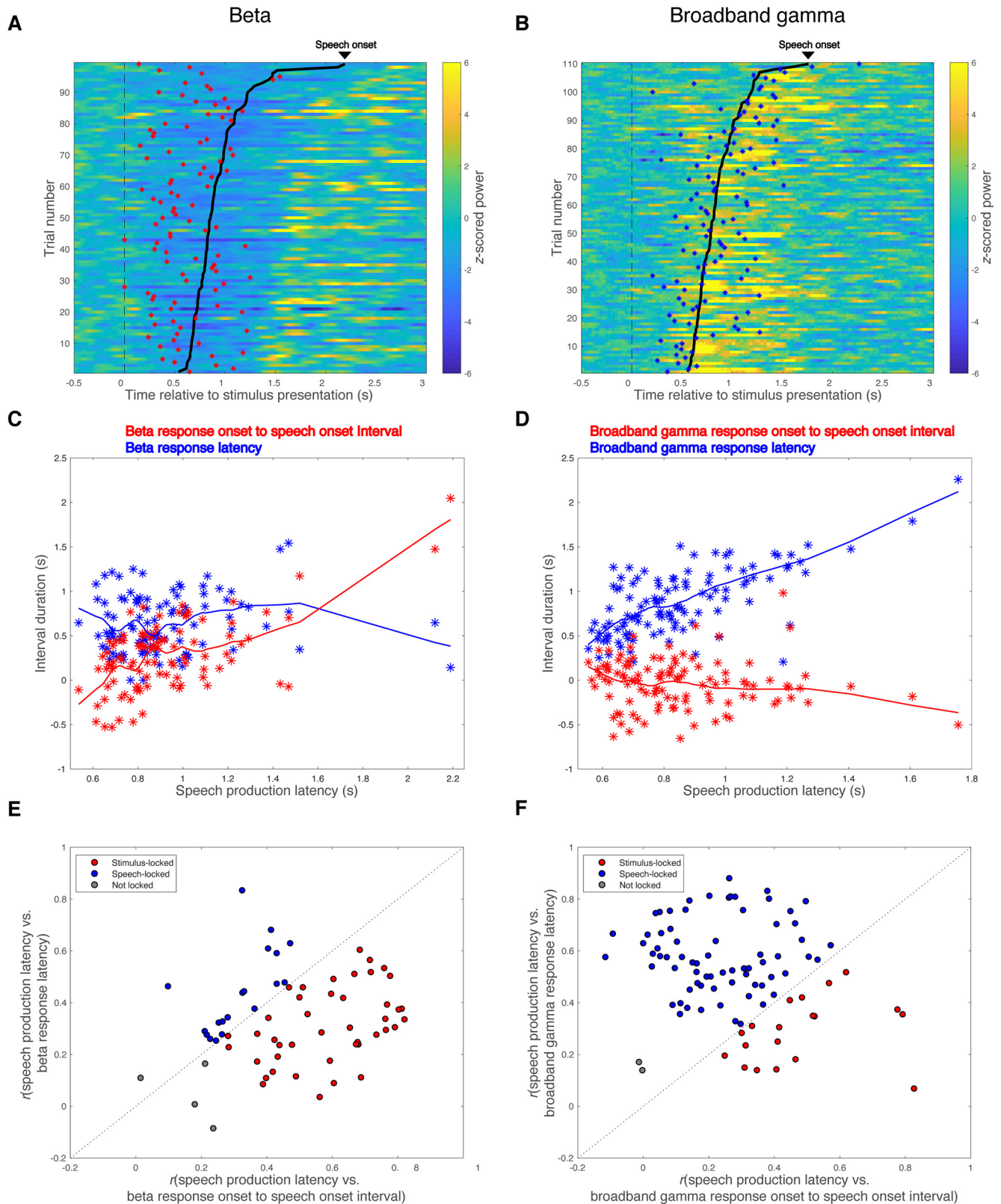


Figure 6. Beta decrease response is time locked to stimulus presentation, whereas broadband gamma increase response is time locked to speech onset. **A**, **B**, Raster plots for beta band responses (**A**) and broadband gamma responses (**B**) across trials of two representative recordings from the VLP of two subjects. Trials are aligned to stimulus presentation (indicated with black dashed lines) and sorted by speech production latency. Speech onsets are denoted with bold black lines. Onsets of significant beta activity decreases are marked with red asterisks in **A**, and onsets of significant broadband gamma activity increases are marked with blue asterisks in **B**. **C**, **D**, Scatter plots showing the relationships between speech production latency and band response onset to speech onset interval (red asterisks) or band response latency (blue asterisks) for the two representative recordings, with LOESS (locally weighted nonparametric regression fitting using a second-order polynomial) lines showing the trends. **E**, **F**, Locking analysis is performed for all the recordings with significant beta decrease responses (**E**) and all the recordings with significant broadband gamma increase responses (**F**). Recordings locked to stimulus presentation are shown in red, recordings locked to speech onset are shown in blue, and recordings not locked to either stimulus presentation or speech onset are shown in gray.

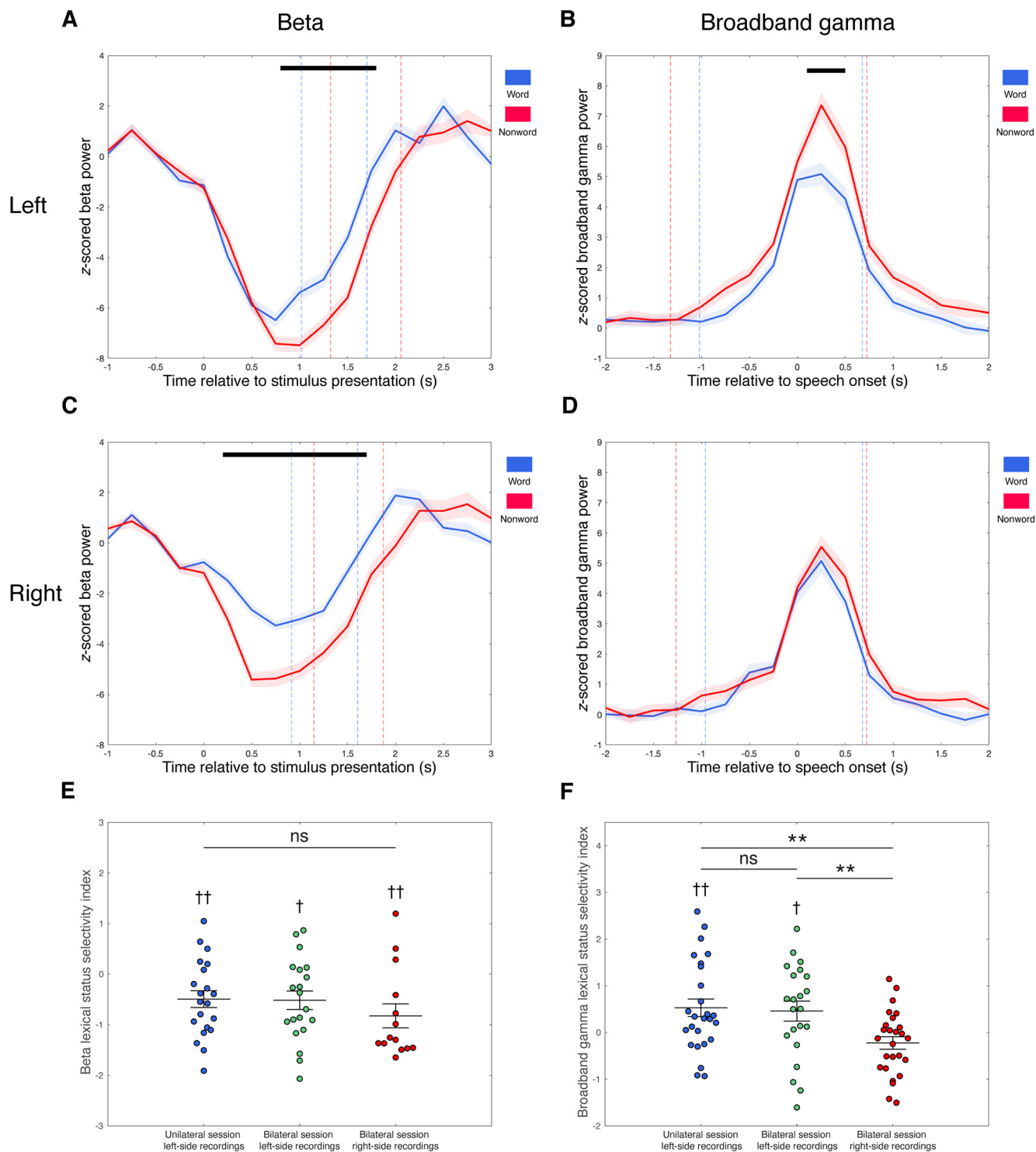


Figure 7. Differential band responses during word versus nonword reading aloud in the left and right thalamus. **A–D**, Comparisons of average band response amplitudes during word (blue) versus nonword (red) reading aloud for beta band (**A**, **C**) and broadband gamma (**B**, **D**) in the left (**A**, **B**) and right (**C**, **D**) thalamus. Band responses are averaged across trials of respective trial types and across recordings that showed significant task-related band responses in each side, aligned to stimulus presentation for beta band (**A**, **C**) and speech onset for broadband gamma (**B**, **D**). Average time points of speech onset and end of speech are marked with dashed lines in **A** and **C**, and average time points of stimulus presentation and end of speech are marked with dashed lines in **B** and **D**, for word trials (blue) and nonword trials (red), respectively. Black bars indicate significant differences of response amplitudes between word and nonword trials (two-tailed paired *t* test, $p < 0.05$, Bonferroni corrected for multiple comparisons across time bins). SEs are shaded in light colors. **E**, Dot plot of beta lexical status selectivity indexes of lead recordings that showed significant task-related beta decrease responses, grouped by recording sides and recording sessions (unilateral session left-side recordings, left column; bilateral session left-side recordings, middle column; and bilateral session right-side recordings, right column). Mean and SE of beta lexical status selectivity index across recordings of each group is superimposed on each column, respectively. **F**, Dot plot of broadband gamma lexical status selectivity indexes of lead recordings that had significant task-related broadband gamma increase responses, grouped by recording sides and recording sessions (unilateral session left-side recordings, left column; bilateral session left-side recordings, middle column; and bilateral session right-side recordings, right column). Mean and SE of broadband gamma lexical status selectivity index across recordings of each group is superimposed on each column, respectively. Two-tailed one-sample *t* test, $\dagger p < 0.05$, $\dagger\dagger p < 0.01$; two-tailed two-sample *t* test, $**p < 0.01$. ns, Not significant.

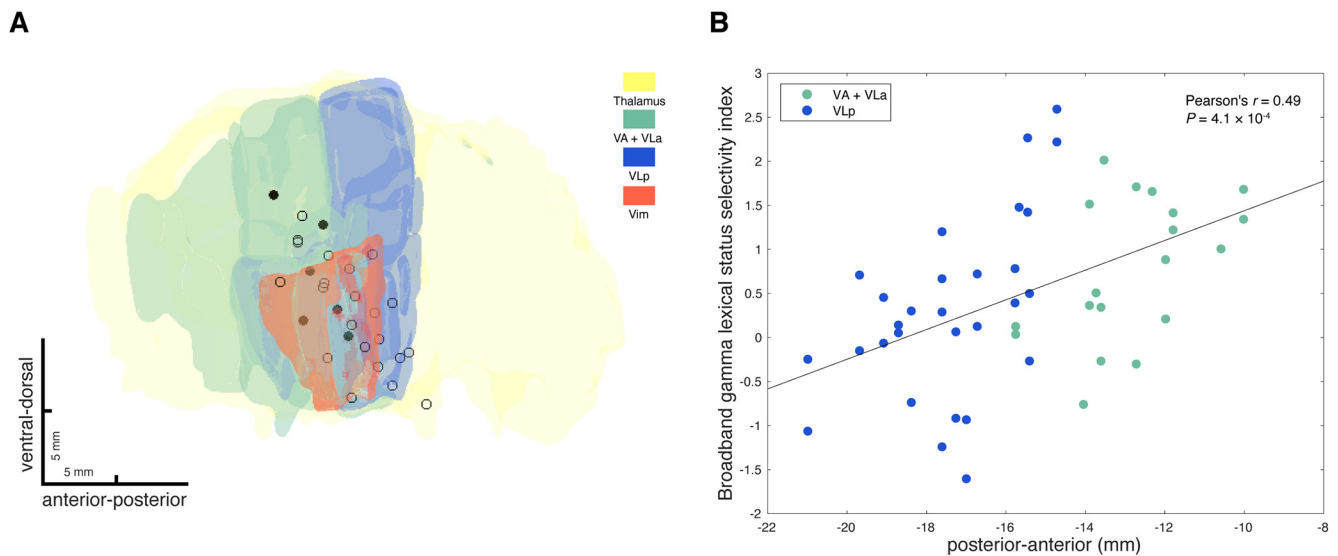


Figure 8. Broadband gamma lexical status selectivity depends on anterior-posterior location of the recording in the left thalamus. **A**, Left side lead recording sites are plotted together with anatomic structures (thalamus in yellow, VA and VL in green, VLp in blue, and Vim in orange), viewed from a lateral direction. Recording sites, where significantly nonword-selective recordings in terms of broadband gamma response amplitudes (broadband gamma lexical status selectivity index greater than 1.645 based on normal approximation of t distribution), were observed in either session are filled with black, and remaining recording sites are shown as open circles. **B**, Broadband gamma lexical status selectivity indexes of left side lead recordings that showed significant task-related broadband gamma responses are correlated (Pearson's correlation) with recording locations along the anterior-posterior axis (y coordinates in MNI space). Recordings inside VA or VL are green colored and recordings inside VLp are blue colored.

space (5/6 sites in VA/VL, 1/6 sites in VLp; Fig. 8A). Pearson's correlation tests demonstrated that the broadband gamma lexical status selectivity index significantly correlated with recording location along the anterior-posterior axis (MNI-defined y coordinate; $n = 48$, $r = 0.49$, $p = 0.00,041$; Fig. 8B) and the ventral-dorsal axis (MNI-defined z coordinate; $n = 48$, $r = 0.30$, $p = 0.041$), but not the lateral-medial axis (MNI-defined x coordinate; $n = 48$, $r = -0.14$, $p = 0.34$) within the left thalamus. To avoid multicollinearity and to test out possible interactions between variables, a stepwise linear regression model was applied, which determined that the anterior-posterior location of the recording was the only significant predictor (estimated coefficient = 0.17, SE = 0.044, $p = 0.00,041$), whereas neither the ventral-dorsal location ($p = 0.72$) nor the interaction between ventral-dorsal location and anterior-posterior location ($p = 0.14$) explained the variance. To control for subject differences and session differences, we further fitted linear mixed-effects models to the data, entering subject and session as random effects. The results indicate that even after accounting for subject and session variability, the broadband gamma lexical status selectivity index in the left thalamus had a significant gradient along the anterior-posterior axis, with greater broadband gamma lexical status selectivity index more likely to be observed anteriorly (estimated coefficient = 0.17, SE = 0.043, $p = 0.00,032$). Based on the linear mixed-effects modeling results, neither ventral-dorsal location (estimated coefficient = 0.061, SE = 0.035, $p = 0.087$) nor lateral-medial location (estimated coefficient = -0.11 , SE = 0.093, $p = 0.24$) of the recording had a significant effect on broadband gamma lexical status selectivity in the left thalamus. Together, these results suggest that broadband gamma lexical status selectivity is dependent on the anterior-posterior location of the recording in the left ventral lateral thalamus, with greater nonword selectivity more likely to occur anteriorly.

No significant correlation between broadband gamma lexical status selectivity index and recording location was observed for right-side recordings or for beta lexical status selectivity on either

side, by any statistical modeling. These results suggest that the topography of lexical status selectivity is unique to broadband beta responses in the left thalamus.

Discussion

Subcortical contributions to language production have been hypothesized largely from correlations of focal brain damage with aphasic syndromes and from language studies using functional magnetic resonance imaging or electrical stimulation (Hebb and Ojemann, 2013). Our results are the first to demonstrate thalamic neural activity during reading aloud, and we discovered that the thalamus participates in lexical status processing in a lateralized and region-specific manner.

We observed that thalamic beta activity showed task-related decreases that were locked to stimulus presentation and were present throughout the entire task event, and these decreases bilaterally were greater when nonwords were read. This beta lexical status selectivity was not region specific within the ventral lateral thalamus. Beta activity decrease during the preparation and the execution stages of various behavioral tasks has been observed across relevant brain regions, including the primary motor and somatosensory cortices, the subthalamic nucleus, and the thalamus (Kühn et al., 2004; Paradiso et al., 2004; Klostermann et al., 2007; Tzagarakis et al., 2010), and it has been thought to signal the change of general sensorimotor or cognitive states (Engel and Fries, 2010). Therefore, thalamic beta activity decreases likely represent nonspecific changes of cognitive and sensorimotor states that prepare the entire thalamo-cortical network for a behavioral change and facilitate the process of speech production. This was further evidenced by our finding that the extent of beta activity decrease was proportional to the task demand (i.e., greater effort required for nonword reading than word reading as indicated by significantly longer speech production latency and speech duration during nonword trials) within the ventral lateral thalamus in both hemispheres. Beta rebound after completion of voluntary movements has been widely

reported (Cao and Hu, 2016). Although conventionally thought to index the return of sensorimotor networks to baseline (Müller et al., 2003), it is now further proposed to signal active maintenance of the current forward model (Cao and Hu, 2016), consistent with the signaling the status quo hypothesis (Engel and Fries, 2010; Cao and Hu, 2016).

Significant increases in thalamic broadband gamma activity began shortly before and were predominantly locked to speech onset and persisted throughout the utterance. As broadband gamma activity is thought to index synchronized local neuronal firing (Ray et al., 2008; Ray and Maunsell, 2011), these data suggest that the ventral lateral thalamus actively tracks speech production. We further found that stronger activation of broadband gamma oscillations was associated with nonword production in the left but not the right hemisphere, and importantly, a topography for this lexicality effect was observed in the left ventral lateral thalamus. The anterior portion, which mainly consists of the VA and VLa, preferentially receives basal ganglia input and has extensive connections with prefrontal cortex including Broca's area (Alexander et al., 1986; Behrens et al., 2003; Zhang et al., 2010; Bosch-Bouju et al., 2013; Hwang et al., 2017; Hintzen et al., 2018) and showed more prominent broadband gamma lexical status selectivity. The dual-route theory of reading aloud has suggested that words and nonwords are read aloud differently; although real words can be read aloud via either grapheme-to-phoneme conversions or direct word-to-sound mapping, nonwords can only be read aloud via grapheme-to-phoneme conversions (Coltheart et al., 2001). The left IFG (Broca's area), a major node subserving both routes (Jobard et al., 2003; Levy et al., 2009; Juphard et al., 2011), is thought to be particularly important in grapheme-to-phoneme conversions, as evidenced by consistently reported greater activation in the IFG during nonword than word reading (Herbster et al., 1997; Fiez et al., 1999; Hagoort et al., 1999; Mechelli et al., 2003; Joubert et al., 2004; Dietz et al., 2005; Heim et al., 2005; Juphard et al., 2011) as well as phonological dyslexia associated with left IFG lesions (Rapcsak et al., 2009; Ripamonti et al., 2014). Therefore, our result suggests that the left VA-VLa may function as a subcortical node of the reading network with a unique role in processing grapheme-to-phoneme conversions by actively modulating IFG activity through thalamo-prefrontal circuits. This is supported by a recent study showing that thalamic aphasia after stroke is exclusively associated with left anterior lesion location (Fritsch et al., 2020). Although the classic speech production model considers orthographic-to-phonological transformation as a process happening before articulation (Levelt et al., 1999), our observation that differential broadband gamma responses between word and nonword trials occurred during the articulatory stage of reading aloud may indicate that there is ongoing grapheme-to-phoneme conversion during articulation, especially for nonword, after a failed internal lexicon lookup procedure. This hypothesis is corroborated by intracerebral EEG data recorded from Broca's area; differential gamma (50–150 Hz) responses were observed between silent pseudo-word versus word reading, which occurred 500 ms after visual stimulus onset and extended beyond the end of the trial, and the duration of gamma responses only increased with pseudo-word length, in direct relation to orthographic-to-phonological conversion (Juphard et al., 2011). Studies of the brain network involved in reading aloud have been confined to cortical regions (Herbster et al., 1997; Fiez et al., 1999; Hagoort et al., 1999; Jobard et al., 2003; Mechelli et al., 2003; Joubert et al., 2004; Dietz et al., 2005; Heim et al., 2005; Levy et al., 2009;

Juphard et al., 2011), and this study is the first to provide direct supporting evidence for thalamic contribution to the reading-aloud network through direct recordings. Indeed, the VA has been proposed to participate in selection of a language unit during speech production, via basal ganglia–thalamo–cortical loop interactions (Crosson, 2013). Future studies should investigate interactions between the thalamus and the IFG through simultaneous recordings from both regions to more clearly delineate thalamic role in this circuit during reading-aloud processes.

In contrast, the posterior region (VLP), which mainly receives cerebellar projections and preferentially sends output to primary motor cortex (Behrens et al., 2003; Zhang et al., 2010; Bosch-Bouju et al., 2013; Hwang et al., 2017; Hintzen et al., 2018), might be more related to motor control of a selected motor plan. This idea is supported by our result that less prominent lexicality effect on broadband gamma activity was observed in this region, as the range of articulatory movements was balanced between word and nonword stimuli. Our finding is also in line with previous stimulation studies that have reported location-dependent effects of thalamic stimulation on speech and language; although stimulation of VLa could cause acceleration of language processes, stimulation of VLP often affected motor aspects of speech, such as perseveration and stuttering speech (Hebb and Ojemann, 2013).

In contrast to these effects seen in the left thalamus, neither broadband gamma lexical status selectivity nor a topography for it was observed in the right thalamus. In concert with previous stimulation and clinical data (Hebb and Ojemann, 2013; Wang et al., 2021), our results from simultaneous bilateral recordings thus further support a lateralized thalamic role in speech and language.

Thalamic function in language has long been implicated in clinical scenarios. Thalamic stroke in the left VA is strongly associated with aphasia (Crosson, 2013; Fritsch et al., 2020), and our previous study has demonstrated that the effect of thalamic DBS on verbal abstraction outcome is dependent on stimulation location within the left ventral lateral thalamus, with stimulation in the anterior portion associated with a worse outcome (Wang et al., 2021). The current electrophysiological data shed light on the neural basis of these clinical findings and emphasize the clinical importance of considering anterior-posterior positioning in Vim DBS, to avoid potential language side effects.

We also observed thalamic delta activity increase during the task. Delta oscillations in the frontal lobe have been associated with inhibition of other processes that interfere with internal concentration during cognitive tasks (Harmony, 2013). Our finding may suggest thalamic involvement in this process, possibly via thalamo-cortical interactions in the delta frequency range, which grants further investigation using simultaneous cortical and thalamic recordings.

It should be noted that in the current work we did not try to compare task-related band response strength between different recording locations and different recording sides among subjects and sessions because of a number of uncontrollable factors that affect the band oscillatory power (e.g., recording impedances and baseline neural activity are variable across subjects, sessions, and recording sides). In contrast, the lexical status selectivity index, which was calculated by comparing word-related and nonword-related band response strength within each recording, is mostly independent of those factors and thus comparable at the group level. This idea is supported by the fact that lexical status

selectivity indexes in both beta and broadband gamma bands remained consistent across sessions.

In summary, our results are the first demonstration of time-frequency modulations of thalamic neural activity during reading aloud. These data suggest that lateralized and topographically organized thalamic pathways participate in reading aloud differently, with a specific thalamic territory in the left hemisphere involved in lexical status processing.

References

- Alexander GE, DeLong MR, Strick PL (1986) Parallel organization of functionally segregated circuits linking basal ganglia and cortex. *Annu Rev Neurosci* 9:357–381.
- Behrens TEJ, Johansen-Berg H, Woolrich MW, Smith SM, Wheeler-Kingshott CAM, Boulby PA, Barker GJ, Sillery EL, Sheehan K, Ciccarelli O, Thompson AJ, Brady JM, Matthews PM (2003) Non-invasive mapping of connections between human thalamus and cortex using diffusion imaging. *Nat Neurosci* 6:750–757.
- Bookheimer SY, Zeffiro TA, Blaxton T, Gaillard W, Theodore W (1995) Regional cerebral blood flow during object naming and word reading. *Hum Brain Mapp* 3:93–106.
- Bosch-Bouju C, Hyland BI, Parr-Brownlie LC (2013) Motor thalamus integration of cortical, cerebellar and basal ganglia information: implications for normal and parkinsonian conditions. *Front Comput Neurosci* 7:163.
- Brainard DH (1997) The psychophysics toolbox. *Spat Vis* 10:433–436.
- Brücke C, Bock A, Huebl J, Krauss JK, Schönecker T, Schneider GH, Brown P, Kühn AA (2013) Thalamic gamma oscillations correlate with reaction time in a Go/noGo task in patients with essential tremor. *Neuroimage* 75:36–45.
- Cao L, Hu Y-M (2016) Beta rebound in visuomotor adaptation: still the status quo? *J Neurosci* 36:6365–6367.
- Chrabaszcz A, Neumann WJ, Stretcu O, Lipski WJ, Bush A, Dastolfo-Hromack CA, Wang D, Crammond DJ, Shaiman S, Dickey MW, Holt LL, Turner RS, Fiez JA, Richardson RM (2019) Subthalamic nucleus and sensorimotor cortex activity during speech production. *J Neurosci* 39:2698–2708.
- Cohen L, Lehericy S, Chochon F, Lemer C, Rivaud S, Dehaene S (2002) Language-specific tuning of visual cortex? Functional properties of the Visual Word Form Area. *Brain* 125:1054–1069.
- Coltheart M, Rastle K, Perry C, Langdon R, Ziegler J (2001) DRC: a dual route cascaded model of visual word recognition and reading aloud. *Psychol Rev* 108:204–256.
- Crone NE, Miglioretti DL, Gordon B, Sieracki JM, Wilson MT, Uematsu S, Lesser RP (1998a) Functional mapping of human sensorimotor cortex with electrocorticographic spectral analysis. I. Alpha and beta event-related desynchronization. *Brain* 121:2271–2299.
- Crone NE, Miglioretti DL, Gordon B, Lesser RP (1998b) Functional mapping of human sensorimotor cortex with electrocorticographic spectral analysis. II. Event-related synchronization in the gamma band. *Brain* 121:2301–2315.
- Crosson B (2013) Thalamic mechanisms in language: a reconsideration based on recent findings and concepts. *Brain Lang* 126:73–88.
- Dietz NAE, Jones KM, Gareau L, Zeffiro TA, Eden GF (2005) Phonological decoding involves left posterior fusiform gyrus. *Hum Brain Mapp* 26:81–93.
- Engel AK, Fries P (2010) Beta-band oscillations—signalling the status quo? *Curr Opin Neurobiol* 20:156–165.
- Ewert S, Plettig P, Li N, Chakravarty MM, Collins DL, Herrington TM, Kühn AA, Horn A (2018) Toward defining deep brain stimulation targets in MNI space: a subcortical atlas based on multimodal MRI, histology and structural connectivity. *Neuroimage* 170:271–282.
- Fiebach CJ, Friederici AD, Müller K, Cramon D. v (2002) fMRI evidence for dual routes to the mental lexicon in visual word recognition. *J Cogn Neurosci* 14:11–23.
- Fiez JA, Balota DA, Raichle ME, Petersen SE (1999) Effects of lexicality, frequency, and spelling-to-sound consistency on the functional anatomy of reading. *Neuron* 24:205–218.
- Fonov V, Evans AC, Botteron K, Almli CR, McKinsty RC, Collins DL (2011) Unbiased average age-appropriate atlases for pediatric studies. *Neuroimage* 54:313–327.
- Fritsch M, Krause T, Klostermann F, Villringer K, Ihrke M, Nolte CH (2020) “Thalamic aphasia” after stroke is associated with left anterior lesion location. *J Neurol* 267:106–112.
- Hagoort P, Indefrey P, Brown C, Herzog H, Steinmetz H, Seitz RJ (1999) The neural circuitry involved in the reading of German words and pseudowords: a PET study. *J Cogn Neurosci* 11:383–398.
- Harmony T (2013) The functional significance of delta oscillations in cognitive processing. *Front Integr Neurosci* 7:83.
- Hebb AO, Ojemann GA (2013) The thalamus and language revisited. *Brain Lang* 126:99–108.
- Heim S, Alter K, Ischebeck AK, Amunts K, Eickhoff SB, Mohlberg H, Zilles K, von Cramon DY, Friederici AD (2005) The role of the left Brodmann’s areas 44 and 45 in reading words and pseudowords. *Brain Res Cogn Brain Res* 25:982–993.
- Herbster AN, Mintun MA, Nebes RD, Becker JT (1997) Regional cerebral blood flow during word and nonword reading. *Hum Brain Mapp* 5:84–92.
- Hintzen A, Pelzer EA, Tittgemeyer M (2018) Thalamic interactions of cerebellum and basal ganglia. *Brain Struct Funct* 223:569–587.
- Horn A, Kühn AA (2015) Lead-DBS: a toolbox for deep brain stimulation electrode localizations and visualizations. *Neuroimage* 107:127–135.
- Horn A, Li N, Dembek TA, Kappel A, Boulay C, Ewert S, Tietze A, Husch A, Perera N, Neumann W-J, Reisert M, Si H, Oostenveld R, Rorden C, Yeh F-C, Fang Q, Herrington TM, Vorwerk J, Kühn AA (2019) Lead-DBS v2: towards a comprehensive pipeline for deep brain stimulation imaging. *Neuroimage* 184:293–316.
- Hwang K, Bertolero MA, Liu WB, D’Esposito M (2017) The human thalamus is an integrative hub for functional brain networks. *J Neurosci* 37:5594–5607.
- Jobard G, Crivello F, Tzourio-Mazoyer N (2003) Evaluation of the dual route theory of reading: a meta-analysis of 35 neuroimaging studies. *Neuroimage* 20:693–712.
- Johnson MD, Ojemann GA (2000) The role of the human thalamus in language and memory: evidence from electrophysiological studies. *Brain Cogn* 42:218–230.
- Joubert S, Beauregard M, Walter N, Bourgouin P, Beaudoin G, Leroux JM, Karama S, Lecours AR (2004) Neural correlates of lexical and sublexical processes in reading. *Brain Lang* 89:9–20.
- Juphard A, Vidal JR, Perrone-Bertolotti M, Minotti L, Kahane P, Lachaux J-P, Baciou M (2011) Direct evidence for two different neural mechanisms for reading familiar and unfamiliar words: an intra-cerebral EEG study. *Front Hum Neurosci* 5:101.
- Klostermann F, Nikulin VV, Kühn AA, Marzinzik F, Wahl M, Pogosyan A, Kupsch A, Schneider G-H, Brown P, Curio G (2007) Task-related differential dynamics of EEG alpha- and beta-band synchronization in cortico-basal motor structures. *Eur J Neurosci* 25:1604–1615.
- Kühn AA, Williams D, Kupsch A, Limousin P, Hariz M, Schneider G-H, Yarrow K, Brown P (2004) Event-related beta desynchronization in human subthalamic nucleus correlates with motor performance. *Brain* 127:735–746.
- Levitt WJM, Roelofs A, Meyer AS (1999) A theory of lexical access in speech production. *Behav Brain Sci* 22:1–75.
- Levy J, Pernet C, Treserras S, Boulanouar K, Aubry F, Démonet JF, Celsis P (2009) Testing for the dual-route cascade reading model in the brain: an fMRI effective connectivity account of an efficient reading style. *PLoS One* 4:e6675.
- Lipski WJ, Alhourani A, Pirnia T, Jones PW, Dastolfo-Hromack C, Helou LB, Crammond DJ, Shaiman S, Dickey MW, Holt LL, Turner RS, Fiez JA, Richardson RM (2018) Subthalamic nucleus neurons differentially encode early and late aspects of speech production. *J Neurosci* 38:5620–5631.
- Llano DA (2013) Functional imaging of the thalamus in language. *Brain Lang* 126:62–72.
- Macchi G, Jones EG (1997) Toward an agreement on terminology of nuclear and subnuclear divisions of the motor thalamus. *J Neurosurg* 86:77–92.
- Mechelli A, Gorno-Tempini ML, Price CJ (2003) Neuroimaging studies of word and pseudoword reading: consistencies, inconsistencies, and limitations. *J Cogn Neurosci* 15:260–271.
- Moore MW, Fiez JA, Tompkins CA (2017) Consonant age-of-acquisition effects in nonword repetition are not articulatory in nature. *J Speech Lang Hear Res* 60:3198–3212.

- Müller GR, Neuper C, Rupp R, Keinrath C, Gerner HJ, Pfurtscheller G (2003) Event-related beta EEG changes during wrist movements induced by functional electrical stimulation of forearm muscles in man. *Neurosci Lett* 340:143–147.
- Oostenveld R, Fries P, Maris E, Schoffelen J-M (2011) FieldTrip: open source software for advanced analysis of MEG, EEG, and invasive electrophysiological data. *Comput Intell Neurosci* 2011:156869–156869.
- Paradiso G, Cunic D, Saint-Cyr JA, Hoque T, Lozano AM, Lang AE, Chen R (2004) Involvement of human thalamus in the preparation of self-paced movement. *Brain* 127:2717–2731.
- Rapcsak SZ, Beeson PM, Henry ML, Leyden A, Kim E, Rising K, Andersen S, Cho HS (2009) Phonological dyslexia and dysgraphia: cognitive mechanisms and neural substrates. *Cortex* 45:575–591.
- Ray S, Maunsell JHR (2011) Different origins of gamma rhythm and high-gamma activity in macaque visual cortex. *PLoS Biol* 9:e1000610.
- Ray S, Crone NE, Niebur E, Franaszczuk PJ, Hsiao SS (2008) Neural correlates of high-gamma oscillations (60–200 Hz) in macaque local field potentials and their potential implications in electrocorticography. *J Neurosci* 28:11526–11536.
- Ripamonti E, Aggajaro S, Molteni F, Zonca G, Frustaci M, Luzzatti C (2014) The anatomical foundations of acquired reading disorders: a neuropsychological verification of the dual-route model of reading. *Brain Lang* 134:44–67.
- Seghier ML, Price CJ (2010) Reading aloud boosts connectivity through the putamen. *Cereb Cortex* 20:570–582.
- Tzagarakis C, Ince NF, Leuthold AC, Pellizzer G (2010) Beta-band activity during motor planning reflects response uncertainty. *J Neurosci* 30:11270–11277.
- Wang D, Jorge A, Lipski WJ, Kratter IH, Henry LC, Richardson RM (2021) Lateralized effect of thalamic deep brain stimulation location on verbal abstraction. *Mov Disord* 36:1843–1852.
- Zhang D, Snyder AZ, Shimony JS, Fox MD, Raichle ME (2010) Noninvasive functional and structural connectivity mapping of the human thalamo-cortical system. *Cereb Cortex* 20:1187–1194.